Particle Size Analysis and Structure of Chromium Hydrous Oxide Sols in the Size Range of Less Than 0.5 μm

Particle size measurements of chromium hydrous oxide sols using electron microscopy and light scattering techniques were in excellent agreement. Comparison was based on the most probable diameter and width of the distribution. The normal, lognormal, and zero-order logarithmic density functions provided good first-order approximations to the particle size measurements. The chromium hydrous sols were less than 0.5 μm in size.

A closed wet cell specimen holder in an electron microscope was developed to observe, in situ, the chromium hydrous oxide sols. The colloidal particles had a uniform spherical shape with a narrow size distribution. Observation of the particle formation process in the closed wet cell qualitatively supports the mechanism that basic polymeric sulfates act as embryos in the formation of these particles.

R. I. LARSON
E. F. FULLAM
A. D. LINDSAY
and E. MATIJEVIĆ

General Electric Company
Knolls Atomic Power Laboratory
Schenectady, New York 12301

SCOPE

Size and concentration of particulate and colloidal material in gases or liquids are important in the control of air and water pollution. The quality of many chemical products and processes such as that found in the food, chemical, pharmaceutical, and power industries is also influenced by particle size. Characterization of small particles in terms of size, shape, chemical nature, and physical structure, therefore, plays an essential role in the solution of many environmental and industrial problems. Measurement of particle sizes above 0.5μm can be accomplished by many techniques such as the Coulter counter, light microscopy, sieve analysis, etc. Particle size measurements below 0.5μm are not easily obtained.

The objective of this study was to measure the particle size distribution of chromium hydrous oxide sols having particle sizes less than 0.5μm and consisting of spherical particles rather uniform in size. Light scattering and electron microscopy techniques were used. The physical structure of these particles, their formation, and growth were also studied, in situ, using a closed wet cell specimen holder in an electron microscope.

Previous light scattering measurements by Kratohvil and Wallace (1970, 1972) and electron microscopy data of Bradford and Vanderhoff (1955) involving polystyrene latex spheres of small diameters were not in agreement. Other authors such as Heard, Wells, and Wiffen (1970) and Megaw and Wells (1968) found similar disagreement when different measuring techniques were used. These discrepancies were attributed to the deformation of the particles by the electron beam. Consequently, comparison of particle size measurement techniques for small particles has met with limited success.

Abrams and McBain (1944) observed volatile liquid media in the electron microscope. However, the nitrocellulose films used in the construction of their closed cell were found to rupture. Higher accelerating voltages of present electron microscopes and improved methods of film formation provided the tools for the development of a more reliable closed wet cell.

CONCLUSIONS AND SIGNIFICANCE

Particle size distribution measurements of chromium hydrous oxide sols using light scattering and electron microscopy methods were in excellent agreement. Comparison was based on the most probable diameter and standard deviation of the colloidal dispersion. Because of experimental error, a clear choice of the detailed shape or form of the distribution function cannot be ascertained. The normal, lognormal and zero-order logarithmic distribution functions are equally good first-order approximations to the narrow size distribution.

Light scattering measurements can be easily performed in situ to provide the particle size distribution of a colloidal suspension. Comparison of these measurements with other techniques such as electron microscopy may indicate deformation of the particles by the electron beam. The agreement of the electron microscopy and light scattering measurements obtained with chromium hydrous oxide sols indicates that such deformations are negligible.

The limitations of the light scattering technique should be recognized. Isotropic spherical particles having a narrow size distribution are required, and the solution must be relatively free from interfering impurities such as dust. Particle size measurements by electron microscopy, on the other hand, are more accurate and can be performed in polydispersed systems having particles of different shapes. Some degree of impurity can also be tolerated, provided individual particle identification is possible. However, sample preparation and the electron beam may

E. F. Fullam is with Ernest F. Fullam, Inc. A. D. Lindsay is with American Cyanamid Company. E. Matijevic is with the Department of Chemistry at Clarkson College of Technology, Potsdam, N. Y.

denature the sol particles.

The closed wet cell specimen holder for the electron microscope confirmed the uniformity, sphericity, and narrow size distribution of chromium hydrous oxide sols. Observation of the formation of these particles in the closed wet cell qualitatively supports the mechanism that basic polymeric sulfates act as embryos in the formation of these particles.

In general, the closed wet cell attachment for an electron microscope can be a useful method for observing, and possibly measuring, in situ, the formation of solid phases from liquids and solutions. This new technique should be of great interest in studying many physical, chemical and biological reactions.

Demchak and Matijević (1969) prepared for the first time a colloidal dispersion of chromium hydrous oxide sols having a narrow size distribution. The monodispersity and sphericity of this sol was established by light scattering measurements using the polarization ratio method described by Kerker et al. (1964) and Jacobsen et al. (1967). Particle size was found to depend on the initial concentration of the starting solution, chrom alum. The existence of such a dispersion has extreme importance in elucidating the mechanisms of particle formation, growth kinetics, and behavior over a wide range of variables such as temperature, *p*H, electrophoretic mobility, stability, chemical additives, etc. Matijević et al. (1971) and Matijević and Bell (1972) describe some studies in this area.

The experimental investigation described in this paper is divided into two phases. In Phase I, a suspension of chromium hydrous oxide sols was prepared according to the procedure outlined by Demchak and Matijević and the particle size distribution measured by electron microscopy. The frequency distribution was compared with the light scattering size distribution measurements of Demchak and Matijević. Good agreement was found. In Phase II electron microscopy and light scattering measurements were performed on the same sample.

EXPERIMENTAL METHODS

Electron Microscopy

In Phase I, a solution of chrom alum, $CrK(SO_4)_2 \cdot 12\ H_2O$, at a concentration of 4×10^{-4} moles/liter was heated for 18 hours at 75°C. Higher order Tyndall spectra (HOTS) were observed, and a narrow size distribution for these chromium hydrous oxide sols was indicated. Drops of the above suspension were air dried on a thin nitrocellulose film supported by a copper grid. Internal magnification calibration was accomplished with a 28,800 line/in. replica. In Phase II, electron microscopy particle size measurements were performed with internal calibration using a 2160 line/mm crossline grating fragment (Figure 1). More than 50 fields were electron micrographed, together with the calibrating line replicas. The electron micrographs were enlarged approximately 3X for a total internally calibrated magnification of 10,000X. Particle size distribution measurements were performed using a Zeiss Particle Analyzer. Experimental uncertainties included:

1. Error in the actual measurement of the grating replicas estimated at less than 0.3% (the more lines measured the less the error).
2. Error due to formation of the grating replicas by the first negative plastic replica—0.3% (a shrinkage of 0.2 and 0.3% may occur).
3. Error caused by the grating replica not being in plane perfectly perpendicular to the optical axis—0.2%.
4. Error in particle size measurement in determining the location of the actual edge of the particle, 3% and 2% in Phase I and II, respectively.

Based on these estimates, the total error in electron microscopy measurements of the average particle size is 4 and 3% in Phases I and II, respectively. The maximum error can be determined from measurements of the smallest particle having a low probability of occurrence. This maximum error was 5.5 and 3.5% in Phase I and II, respectively.

Light Scattering

Particle size distribution data were obtained from light scattering measurements using the polarization ratio and specific intensity methods. These two techniques are based on the Mie scattering theory for an isolated particle in an infinite medium described by Kerker et al. (1964), Kerker (1969), and Van de Hulst (1957). The total scattered energy that is measured is equal to the energy scattered by one sphere multiplied by their number. To minimize the interference of the scattered radiation among the individual wavelets and to avoid multiple scattering, experimental data were obtained at several concentrations and extrapolated to infinite dilution.

Both the polarization ratio and specific intensity methods can be expressed in terms of the Rayleigh ratios ($V_{\theta,v}$ and $H_{\theta,h}$) of scattered intensity per unit angle from an incident beam of unit irradiance, that is,

$$V_{\theta,v} = N(\lambda/2\pi)^2 \int (i_1)_\theta\, p\,(\alpha)\, d\alpha \qquad (1)$$

$$H_{\theta,h} = N(\lambda/2\pi)^2 \int (i_2)_\theta\, p\,(\alpha)\, d\alpha \qquad (2)$$

In the above equations, $p\,(\alpha)$ is the probability density function. $(i_1)_\theta$ and $(i_2)_\theta$ are the vertical and horizontal angular intensity functions obtained by direct computation from the Mie scattering theory and depend on the relative refractive index.

The polarization ratio method eliminates the need for calibration and correction factors of the Brice-Phoenix light scattering photometer. Usually, the polarization of scattered radiation is measured at 19 angles of observation and several con-

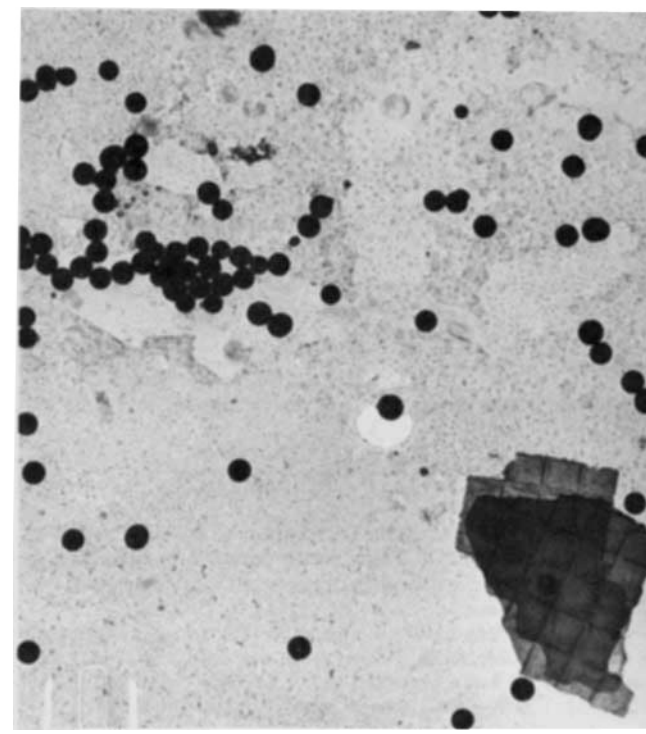

Fig. 1. Crossline grating replica and spherical chromium hydrous oxide particles, 20,000X.

TABLE 1. LIGHT SCATTERING PARTICLE SIZE MEASUREMENTS

Wave length: $\lambda_0 = 0.546\ \mu m$

Method	α_m	σ_0	$D_{pm}(\mu m)$
Polarization ratio[1]	2.22	0.12	0.289
Polarization ratio[2]	2.22	0.12	0.289
Specific intensity[3]	2.21	0.10	0.287
Specific intensity[4]	2.23	0.12	0.291

Wave length: $\lambda_0 = 0.436\ \mu m$

Method	α_m	σ_0	$D_{pm}(\mu m)$
Polarization ratio[1]	2.89	0.10	0.301
Polarization ratio[2]	2.90	0.10	0.302
Specific intensity[3]	2.92	0.07	0.304
Specific intensity[4]	2.90	0.09	0.302

[1] $\rho(\theta)$—concentration curves extrapolated to zero to determine $\rho_0(\theta)$, α_m, and σ_0 at infinite dilution.

[2] α_m and σ_0 determined at each concentration and extrapolated to zero to obtain the values of α_m and σ_0 at infinite dilution.

[3] $V_{\theta,v}/C$ and $H_{\theta,h}/C$ plotted against concentration and extrapolated to zero to obtain $\rho_0(\theta)$, α_m, and σ_0 at infinite dilution.

[4] $\rho(\theta)$ determined from specific intensities is plotted against concentration, extrapolated to zero, and $\rho_0(\theta)$, α_m, and σ_0 determined at infinite dilution.

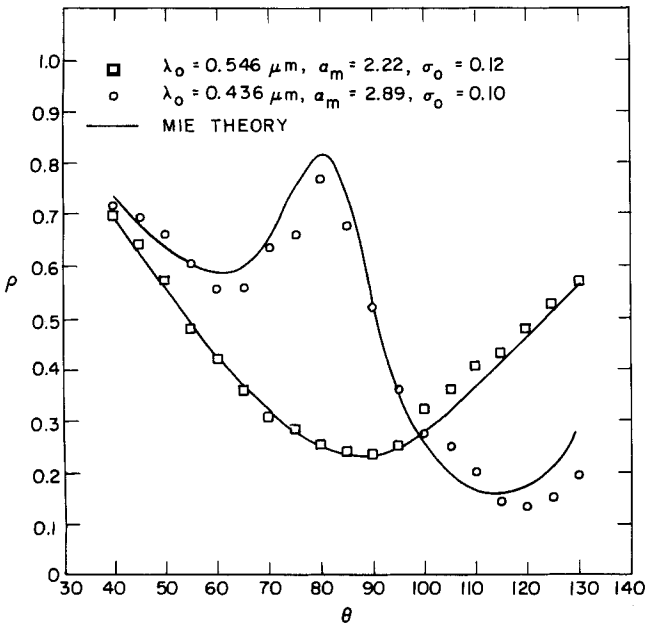

Fig. 2. Comparison of experimental and theoretical polarization ratios.

centrations. These results are analyzed using the following expression:

$$\rho(\theta) = \frac{H_{\theta,h}}{V_{\theta,v}} = \frac{\int (i_2)_\theta\, p(\alpha)\, d\alpha}{\int (i_1)_\theta\, p(\alpha)\, d\alpha} \qquad (3)$$

The zero-order logarithmic distribution is assumed for $p(\alpha)$ in the data analysis. This distribution function is described in the appendix and compared to the normal and lognormal distribution functions.

Because the maximum in the $\rho(\theta)$ curves is exaggerated relative to the minimum, inversion of the light scattering data is accomplished more accurately by using the degree of polarization $P(\theta)$ rather than the polarization ratio $\rho(\theta)$ where

$$P(\theta) = \frac{\rho(\theta) - 1}{\rho(\theta) + 1} \qquad (4)$$

The degree of polarization $P(\theta)$ is compared to the experimental data to determine the size distribution parameters α_m and σ_0. The polarization ratio was measured at four concentrations and extrapolated to infinite dilution to obtain $\rho_0(\theta)$ values for comparison with the Mie theory. A second method of analyzing the polarization ratio data involved calculation of the size distribution parameters at each concentration and extrapolation of these parametric values to zero.

Specific intensities $H_{\theta,h}/C$ and $V_{\theta,v}/C$ were also analyzed by two methods. First, the specific intensities at a given angle were extrapolated to infinite dilution and the absolute specific intensities $(H_{\theta,h}/C)_{c=0}$ and $(V_{\theta,v}/C)_{c=0}$ obtained. Using the polarization ratio, the size distribution parameters were determined. A second method of analyzing the specific intensity data calculated the polarization ratio at each concentration and extrapolated the $\rho(\theta)$ values to infinite dilution. The results of the polarization ratio and specific intensity methods are summarized in Table 1.

The theoretical values of Mie light scattering functions (expressed as ρ, P, V and H) were calculated as a function of the angle (θ) assuming the zero-order logarithmic distribution for a range of modal diameters and σ_0. A relative refractive index of 1.22 was used in the calculation. The size distribution parameters are determined from the best fit of the light scattering data. Figure 2 shows the best fit of the theoretical and experimental data for wavelengths of 0.546 μm and 0.436 μm.

Analysis of Phase II light scattering results gave a maximum error of 2.5% in the modal diameter and a corresponding maximum error of 30% in σ_0. These results agreed with Demchak and Matijevic (1969) and Jacobsen et al. (1967) error contour maps, showing that a 2 to 3% error in the modal diameter corresponded to a 20 to 40% error in σ_0.

Closed Wet Cell Specimen Holder for the Electron Microscope

A closed wet cell was developed for the 120 KV Jeolco electron microscope to establish the sphericity and uniformity of the chromium hydroxide sols. Further description is presented by Fullam (1972). The solution to be examined is retained between the 400 mesh electrolytic copper screens, covered with Formvar, nitrocellulose, and silicon monoxide films. The two plastic films seal any holes and provide a continuous substrate for the deposition of silicon monoxide film. The pair of triple films retain volatile liquids in the vacuum of the electron microscope.

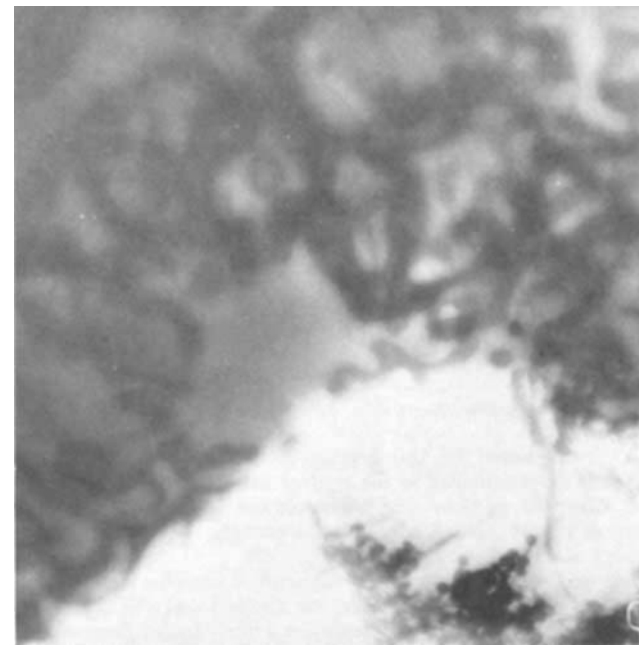

Fig. 3a. Stages in the formation of spherical particles—chrom alum solution, 4000X.

RESULTS

Formation of Spherical Particles

Hall and Eyring (1950) previously investigated chromium salt solutions and found that heating led to the formation of polymeric species. Demchak and Matijević (1969) hypothesized that such polymeric basic sulfates act as embryos in the process of particle formation. Using the wet cell, it became possible to follow the process of particle nucleation and growth. Sequential electron micrographs of the chrom alum solution being heated by the electron beam in the closed wet cell were obtained.

Figure 3a shows a drop of the chrom alum solution shortly after being placed in the wet cell. Because of the

Fig. 3b. Stages in the formation of spherical particles—polymeric species formed during evaporation, 4000X.

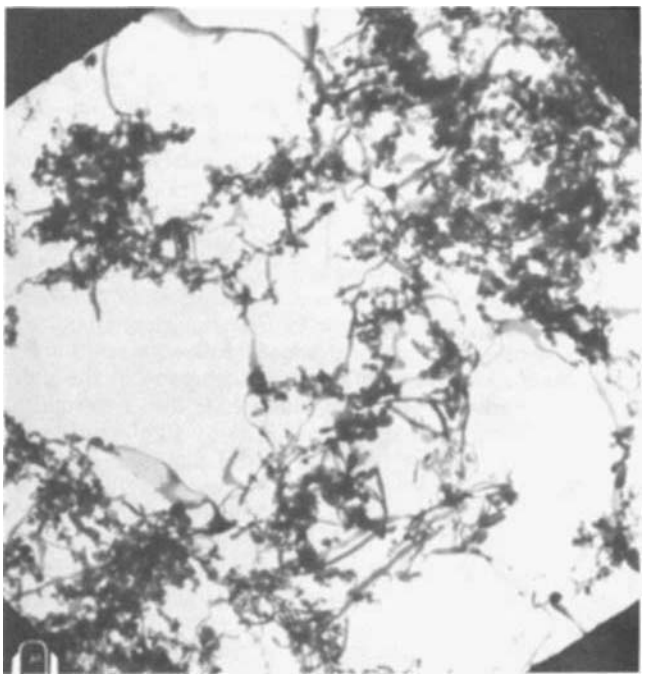

Fig. 3c. Stages in the formation of spherical particles—initial formation of spherical particles, 4000X.

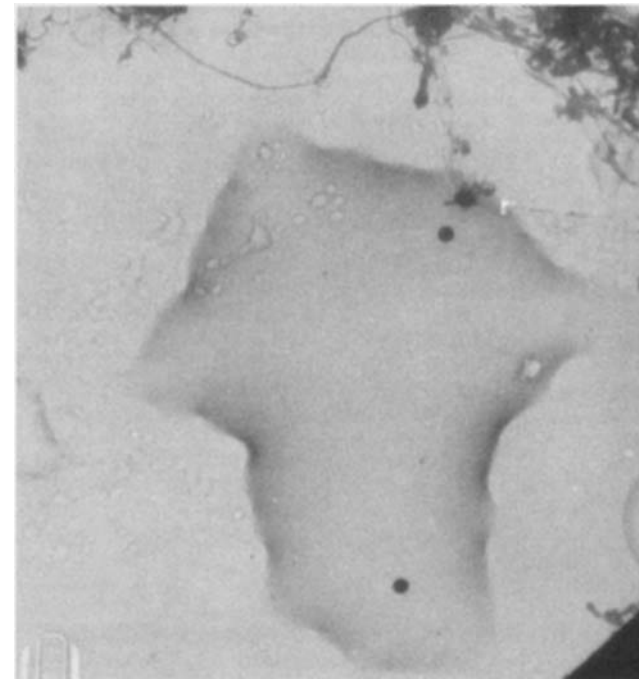

Fig. 3d. Stages in the formation of spherical particles—spherical particles forming in water droplet, 4000X.

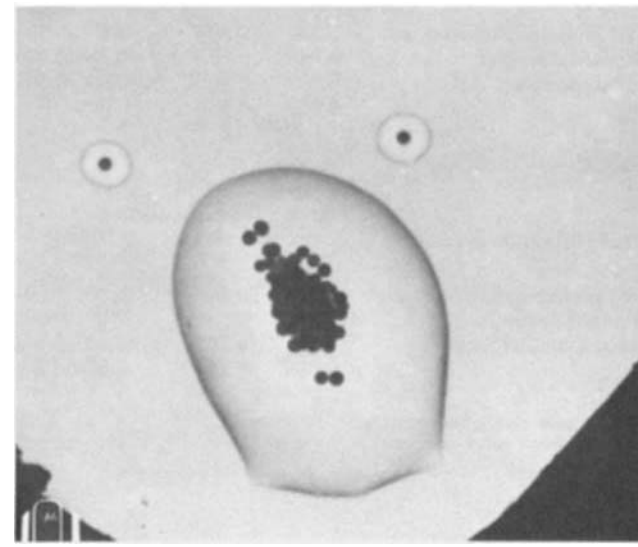

Fig. 3e. Spherical particles suspended in water droplet—7200X.

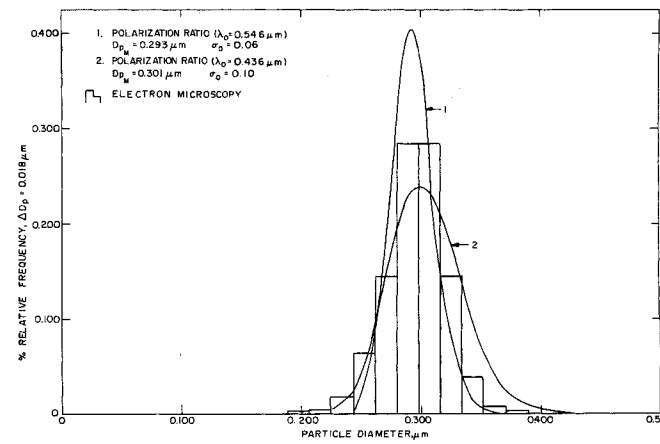

Fig. 4. Particle size distribution measurements (Phase I).

TABLE 2. ELECTRON MICROSCOPY PARTICLE SIZE MEASUREMENTS

Phase I		Phase II	
D_p μm	No. of particles	D_p μm	No. of particles
0.197	4.0	0.1975	1.0
0.215	10.0	0.2084	5.0
0.234	41.0	0.2193	8.0
0.252	144.0	0.2309	29.0
0.270	327.0	0.2418	45.0
0.289	639.0	0.2533	86.0
0.307	639.0	0.2642	155.0
0.326	327.0	0.2751	227.0
0.344	89.0	0.2866	266.0
0.326	19.0	0.2975	272.0
0.381	6.0	0.3090	182.0
0.399	1.0	0.3200	92.0
		0.3309	19.0
		0.3424	7.0

TABLE 3. COMPARISON OF ELECTRON MICROSCOPY AND LIGHT SCATTERING RESULTS

Phase I

Size distribution parameter	Electron micros-copy	Light scattering Average	Range
Most probable diameter, μm	0.298	0.297	0.293-0.301
Standard deviation	0.026	0.024(2)	0.018-0.030
Modal diameter, μm(1)	0.293	0.297	0.293-0.301
σ_0	0.089	0.08	0.06-0.10

Phase II

Size distribution parameter	Electron micros-copy	Light scattering Average	Range
Most probable diameter, μm	0.298	0.296	0.287-0.304
Standard deviation	0.025	0.030(2)	0.021-0.035
Modal diameter, μm(1)	0.281	0.296	0.287-0.304
σ_0	0.086	0.10	0.07-0.12

(1) Assumes zero-order logarithmic distribution.
(2) Calculated using appendix Equation (A7).

movement of solid material suspended in the solution, resolution is poor. Strands of polymeric material are formed as water evaporates (Figure 3b) and eventually spherical particles appear as the polymeric strands are reduced in size (Figure 3c). Figure 3d shows two perfect spheres in a water droplet immediately below the polymeric material. In the upper portion of the water droplet, a spherical particle appears to be in the process of formation originating from the strands of polymeric material.

Figure 3e shows the chromium hydrous oxide sols in their final spherical form suspended in water after heating the chrom alum solution for 18 hours at 75°C. The spheres are uniform and spherical in shape as the light scattering measurements had indicated. A narrow size distribution is also observed.

Comparison of Particle Size Distribution Measurements

Particle size measurements by light scattering and electron microscopy are summarized in Table 1 and 2, respectively. Size distribution parameters are compared in Table 3. The modal diameters measured by electron-microscopy are in excellent agreement with the average

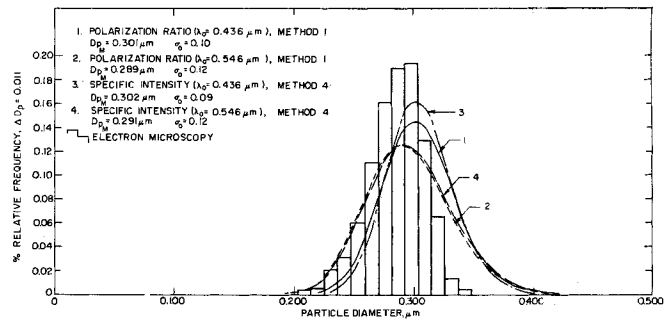

Fig. 5. Particle size distribution measurements (Phase II).

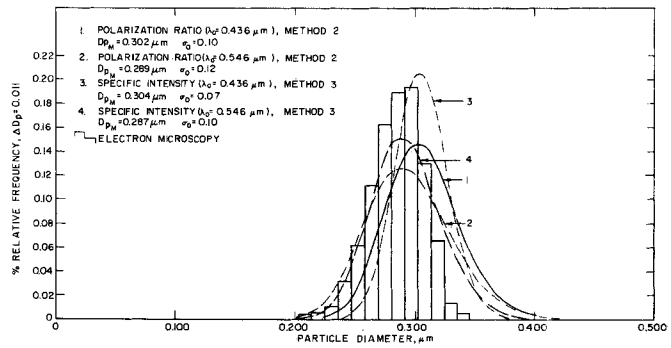

Fig. 6. Particle size distribution measurements (Phase II).

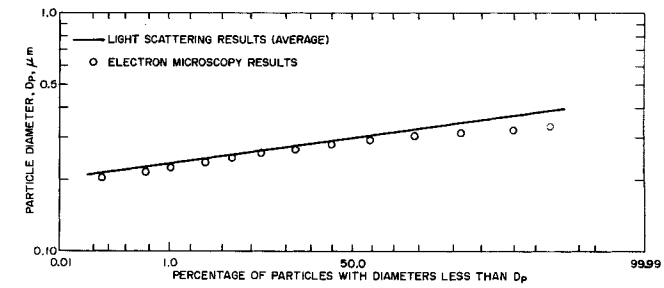

Fig. 7. Cumulative distribution curve electron microscopy and light scattering results (Phase II).

modal diameter obtained by light scattering. The width of the distribution as indicated by either the standard deviation or σ_0 is also in good agreement.

Figures 4, 5, and 6 present the relative frequency curves of the light scattering and electron microscopy results. A cumulative distribution plot is shown in Figure 7. Good agreement of the two measurement techniques is observed. Some of the variation in the two measurements can be attributed to the form of the distribution function.

For example, if it is assumed that the electron microscopy particle size measurements follow a zero-order logarithmic distribution* (a priori assumption of the light scattering results), the modal diameter is 3 to 7% smaller than the modal diameter determined by light scattering; and 2 to 6% smaller than the modal diameter obtained directly from the electron microscopy histograms (See Table 3 and Figure 8). The left skewness of the electron microscopy histograms causes this difference. Furthermore, as shown in the cumulative distribution plot, Figure 7, the light scattering and electron microscopy results

* The modal or most probable diameter is one of the two parameters in the zero-order logarithmic density function. (See appendix for discussion)

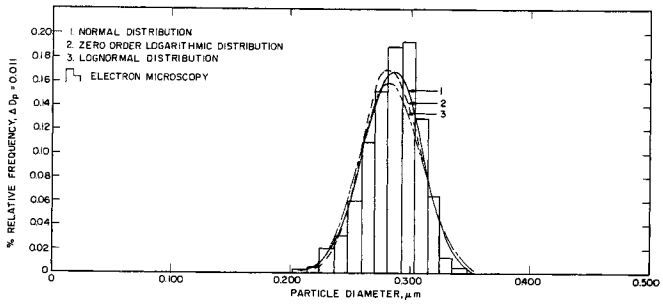

Fig. 8. Comparison of electron microscopy results with different probability density functions.

depart at large diameters due to the left skewness of the electron microscopy histogram.

If the electron microscopy measurements are approximated by normal or lognormal density functions (Figure 8), skewness towards smaller diameters reduces the calculated modal diameter. Consequently, the two parameter distribution functions are good first-order approximations to the electron microscopy results but tend to underestimate the modal diameter.

Wallace and Kratohvil (1972) found the light scattering method to be incapable of detecting the presence or absence of a slight skewness in either direction. However, the agreement between the electron microscopy and light scattering parameters show that these two parameter density functions are good first-order approximations to the narrow size distribution of chromium hydrous oxide sols.

NOTATION

$\overline{D_p}$ = mean particle diameter
D_{pg} = geometric mean particle diameter
D_{pm} = modal diameter
H_θ = scattered intensity of the horizontal component at angle θ
$(i_1)_\theta$ = Mie angular intensity function at infinite dilution for vertical polarized component of light
$(i_2)_\theta$ = Mie angular intensity function at infinite dilution for horizontal polarized component of light
N = number of particles per unit volume
$p(D_p)$ = normal, logarithmic normal, or zero order logarithmic distribution
P = degree of polarization
V_θ = scattered intensity of the vertical component at angle θ

Greek Letters

α = size parameter $= \pi D_p/\lambda$
α_m = modal size parameter, $\pi D_{pm}/\lambda$
λ_0 = wave length in vacuum
λ = wave length in the medium
ρ = polarization ratio
σ = standard deviation
σ_g = standard geometric deviation
σ_0 = width parameter for zeroth order logarithmic distribution
θ = infinite dilution conditions

Subscripts

v = perpendicular polarized component of incident radiation
h = horizontal polarized component of incident radiation
0 = infinite dilution conditions

LITERATURE CITED

Abrams, I. M., and J. W. McBain, "A Closed Cell for Electron Microscopy," *J. Appl. Phys.*, **15**, 607 (1944).

Bradford, E. B., and J. W. Vanderhoff, "Electron Microscopy of Monodisperse Latexes," *ibid.*, **26**, 864 (1955).

Demchak, R., and E. Matijevic, "Preparation and Particle Size Analysis of Chromium Hydroxide Hydrosols of Narrow Size Distribution," *J. Colloid Interfac. Sci.*, **31**, 257 (1969).

Espenscheid, W. F., M. Kerker, and E. Matijevic, "Logarithmic Distribution Function for Colloidal Particles," *J. Phys. Chem.*, **68**, 309 (1964).

Fullam, E. F., "A Closed Wet Cell for the Electron Microscope," *Rev. Sci. Instr.*, **43**, 245 (1972).

Hall, H. T., and H. Eyring, "The Constitution of Chromic Salts in Aqueous Solution," *J. Am. Chem. Soc.*, **72**, 782 (1950).

Heard, M. J., A. C. Wells, and R. D. Wiffen, "A Re-Determination of the Diameter of Dow Polystrene Latex Spheres," *Atm. Environ.*, **4**, 149 (1970).

Jacobson, R. J., M. Kerker, and E. Matijevic, "Aerosol Studies by light Scattering. V. Preparation and Particle Size Distribution of Aerosols Consisting of Particles Exhibiting High Optical Absorption," *J. Phys. Chem.*, **71**, 514 (1967).

Kerker, M., *The Scattering of Light and Other Electromagnetic Radiation*, Academic Press, New York (1969).

———., E. Matijevic, W. F. Espenscheid, W. A. Farone, and S. Kitani, "Aerosol Studies By Light Scattering, I. Particle Size Distribution By Polarization Ratio Method," *J. Colloid Sci.*, **19**, 213 (1964).

Kratohvil, J. P., and T. P. Wallace, "Calibration of Light Scattering Photometers VII. Calibration by Means of Colloidal Dispersions of Mie Scatters," *Appl. Phys.* (London) **3**, 221 (1970).

Matijevic, E., A. D. Lindsay, S. Kratohvil, M. E. Jones, R. I. Larson, and N. W. Cayey, "Characterization and Stability of Chromium Hydroxide Sols of Narrow Size Distribution," *J. Colloid Interfac. Sci.*, **36**, 273 (1971).

Matijevic, E., and A. A. Bell, "Formation and Growth of Chromium Hydroxide Hydrosols of Narrow Size Distribution," *Soc. Chem. Ind.* (London), in press.

Megaw-W. J. and A. C. Wells, "Electrical Mobility of Submicron Particles," *Nature* (Lond.), **219**, 259 (1968).

Van de Hulst, H. C., *Light Scattering By Small Particles*, Wiley, New York (1957).

Wallace, T. P., and J. P. Kratohvil, "Particle Size Analysis of Polymer Latexes by Light Scattering. V. The Significance of an Assumed Distribution in the Analysis of Angular Scattering Data," *J. Polym. Sci.*, **A2**, 631 (1972).

———., "Particle Size Analysis of Polymer Latexes by Light Scattering II. Computer Analysis," *ibid.*, **C25**, 89 (1968).

APPENDIX. PARTICLE SIZE DISTRIBUTION FUNCTIONS

The best known probability density function is the normal distribution

$$p(D_p) = \frac{1}{(2\pi)^{1/2}\,\sigma} \exp\left[-\frac{(D_p - \overline{D_p})^2}{2\sigma^2}\right] \quad \text{(A1)}$$

where $\overline{D_p}$ is the mean particle diameter and σ is the standard deviation of the diameter. The normal distribution curves are symmetrical, thereby allowing for negative values of D_p. This introduces a negligible error provided the standard deviation is small compared to the mean diameter. Because of symmetry, the modal, mean, and median diameters are identical.

A large number of natural occurring processes, however, are asymmetric with a steeper slope on the side of small diameters. One possible representative of such a population is the logarithmic normal distribution:

$$p(D_p) = \frac{1}{(2\pi)^{1/2}\,\sigma_g\,D_p} \exp\left[-\frac{(\log D_p - \log D_{pg})^2}{2\sigma_g^2}\right] \quad \text{(A2)}$$

where D_{pg} is the geometric mean or median value of D_p. σ_g is the standard deviation of log D_p and is called the standard

geometric deviation. The skewness of the distribution depends on the value of σ_g. At small values the skewness is reduced and the frequency curve approximates the normal distribution.

To obtain the fraction of particles between D_p and $D_p + dD_p$ the above probability density functions are integrated as indicated below:

$$P(D_{pi} < D_p < D_{pi} + dD_p) = F(D_{pi} + dD_p) - F(D_{pi}) \quad \text{(A3)}$$

$$= \int_{D_{pi}}^{D_{pi}+D_p} p(\xi)\, d\xi$$

where

$$F(D_p) = \int_{\infty}^{D_p} p(\xi)\, d\xi$$

and

$$\int_{-\infty}^{\infty} p(D_p)\, dD_p = 1$$

Some authors have modified the logarithmic density function by eliminating the diameter D_p in the denominator of Equation (A2).

$$p(D_p) = \frac{1}{(2\pi)^{1/2}\sigma_0} \exp\left[-\frac{(\log D_p - \log D_{pm})^2}{2\sigma_0^2}\right] \quad \text{(A4)}$$

Normalization of this equation leads to the zero-order logarithmic distribution function:

$$p(D_p) = \frac{\exp\left[-\dfrac{(\log D_p - \log D_{pm})^2}{2\sigma_0^2}\right]}{(2\pi)^{1/2}\sigma_0 D_{pm} \exp\left[\dfrac{\sigma_0^2}{2}\right]} \quad \text{(A5)}$$

This distribution is defined by two parameters: the modal diameter, D_{pm} and σ_0. D_{pm} can be expressed in terms of the mean diameter as shown below:

$$\ln \overline{D}_p = \ln D_{pm} + 1.5\,\sigma_0^2 \quad \text{(A6)}$$

and the standard deviation is related to σ_0 by the following equation:

$$\sigma = D_{pm}[\exp(4\sigma_0^2) - \exp(3\sigma_0^2)]^{1/2} \quad \text{(A7)}$$

Espenscheid et al. (1964) and Kerker (1969) describe some of the properties of the zero-order logarithmic distribution, which is used in analyzing the light scattering measurements by either the polarization ratio of specific intensity methods.

Manuscript received July 10, 1972; revision received January 26, 1973, and accepted January 29, 1973.

Enhancement of Stagnation Flow Heat and Mass Transfer Through Interactions of Free Stream Turbulence

At the forward stagnation point of a bluff body the laminar flow is influenced by externally generated free-stream turbulence, such as from grids, in such a way that heat and mass transport are significantly enhanced above their normal values. The basis of this enhancement is an unsteady, three-dimensional flow pattern formed at the forward stagnation point and triggered or altered by the free-stream turbulence. Such complex flows can be interpreted as roll cells oriented with their axes parallel to streamwise coordinates. Such roll cells have been observed by other investigators using special experimental visualization techniques. This complex flow was introduced into the momentum and transport equations, which were then solved numerically to produce the relationships between Nusselt, Reynolds, and Prandtl numbers and free-stream turbulence. Not only were these relationships nearly identical with earlier established empirical correlations, but they revealed in addition a strong augmentation for high Prandtl number flows. Predictions in slurry flows around bluff bodies were also found to be reasonable.

T. R. GALLOWAY

University of California
Berkeley, California

SCOPE

One of the most commonly encountered problems in the chemical and petroleum process industries is that of heat or mass transfer from a cylindrical or spherical surface to the fluid flowing past it. The cylinders can be heat exchanger tubes, column packing, catalyst pellets, etc., and spheres can be droplets, bubbles, bed or catalyst packing, etc. The fluid can be gas or liquid and can contain particulates of solid or other phases. In nearly all these cases the

T. R. Galloway is Assistant Director of the Sanitary Engineering Research Laboratory, Richmond Field Station, Richmond, California 94804.